Prof. Mieczyslaw JURCZYK, (Ph.D., D.Sc.), Marek NOWAK, (Ph.D.)
Katarzyna NIESPODZIANA, (M.Sc.), Maciej TULINSKI, (M.Sc.)
Poznan University of Technology, Institute of Materials Science and Engineering, Poznan, Poland

Metallic nanomaterials for advanced applications

Zastosowanie nanomateriałów metalicznych

Abstract
This paper reviews research at the Institute of Materials Science and Engineering, Poznań University of Technology, on the synthesis of nanoscale metallic materials. These materials were prepared by the combination of mechanical alloying and powder metallurgical process. Examples of the materials include a titanium-hydroxyapatite nanocomposite, a nanocrystalline nickel-free stainless steels, both for biomedical applications, and molybdenum disulfide (MoS_2) nanoparticles for engineering applications. The results show an enhancement of properties due to the nanoscale structures in bulk consolidated materials.

Streszczenie
Artykuł jest przeglądem badań prowadzonych w Instytucie Inżynierii Materiałowej Politechniki Poznańskiej nad otrzymywaniem materiałów metalicznych z nanostrukturą. Materiały te otrzymywane są metodą mechanicznej syntezy a następnie konsolidowane za pomocą technologii metalurgii proszków. Przykładami otrzymanych nanomateriałów są: nanokompozyt tytan – hydroxyapatyt, nanokrystaliczna bez niklowa stal nierdzewna, mające zastosowanie jako biomateriały, oraz dwusiarczek molibdenu (MoS_2) w postaci nanocząstek mający zastosowanie w materiałach inżynierskich. Wynik badań pokazują, iż materiały posiadające nanostrukturę wykazują lepsze właściwości w porównaniu do materiałów tradycyjnych.

Key words: nanoscale materials; Ti-HA nanocomposite; Ni-free austenitic stainless steels; molybdenum disulfide (MoS_2)

Słowa kluczowe: *materiały w nanoskali; nanokompozyt Ti-HA; bezniklowe stale austenityczne; dwusiarczek molibdenu (MoS_2)*

1. INTRODUCTION

In 1959 Professor Feynman presented his famous idea of nanostructured materials production. He suggested that combination of single atoms could lead to formation of new special materials with unconventional properties. Today, it is possible to prepare metal/alloy nanocrystals with nearly monodispersive size distribution. Nanostructures represent key building blocks for nanoscale science and technology. They are needed to implement the "bottom-up" approach to nanoscale fabrication, whereby well-defined nanostructures with unique properties are assembled into mechanical as well as functional properties.

During last years, interest in the study of nanostructured materials has been increasing at an accelerating time, stimulated by recent advances in materials synthesis and characterization techniques and the realization that these materials exhibit many interesting and unexpected physical, chemical as well as mechanical properties with a number of potential technological applications. For example, magnetic and hydrogen storage nanomaterials are the key to the future of the storage and batteries/cells industries [1-3]. On the other hand, the recent development of nanostructured alloys, the demand for higher microhardness and the emergence of completely new technologies call for entirely new type of engineering nanomaterials with much higher mechanical properties [4-6].

Since 1996 a research program was initiated at Institute of Materials Science and Engineering, Poznań University of Technology in which fine grained, intermetallic compounds were produced by mechanical allying (MA) [1,7,8]. The mechanical synthesis of nanopowders and their subsequent consolidation is an example how this idea can be realized in metals by so called bottom-up approach. On the other hand, other methods have been developed, which are based on the concept of the production of nanomaterials from conventional bulk materials via top-down approach. The investigations by severe plastic deformation (e.g. cyclic extrusion compression method (CEC) or equal channel angular extrusion (ECAE)), show that such a transformation is indeed possible.

The main objective of the present paper is to review the advantages of some nanomaterials, their application in various fields and the challenges involved in their fabrication. Details of the processing used and the enhancement of properties due to the nanoscale structures in consolidated materials are presented. The measurements of the properties are also included.

2. MECHANICAL ALLOYING

Grain refinements to a nanoscale range open up possibilities of a considerable decrease in temperatures for compaction or super-plastic forming as the rates of these diffusion related processes increase dramatically when the grain or particle size decreases. Currently, in our laboratory the following technologies have been used to produce nanocrystalline metal/alloy powders as well nanocomposites: mechanical alloying, MA, high energy ball milling, HEBM.

Mechanical alloying was developed in the 1970's at the International Nickel Co as a technique for dispersing nanosized inclusions into nickel-based alloys [9]. During the last years, the MA process has been successfully used to prepare a variety of alloy powders including powders exhibiting supersaturated solid solutions, quasicrystals, amorphous phases and nano-intermetallic compounds [10]. MA technique has been proved a novel and promising method for alloy formation.

The raw materials used for MA are available commercially high purity powders that have sizes in the range of 1-100 μm. During the mechanical alloying process, the powder particles are periodically trapped between colliding balls and are plastically deformed. Such a feature occurs by the generation of a wide number of dislocations as well as other lattice defects. Furthermore, the ball collisions cause fracturing and cold welding of the elementary particles, forming clean interfaces at the atomic scale. Further milling lead to an increase of the interface number and the sizes of the elementary component area decrease from millimeter to submicrometer lengths. Concurrently to this decrease of the elementary distribution, some nanocrystalline intermediate phases are produced inside the particles or at its surfaces. As the milling duration develops, the content fraction of such intermediate compounds increases leading to a final product whose properties are the function of the milling conditions.

It was shown, that mechanical alloying have produced amorphous phases in metals. But differentiation between a „truly" amorphous, extremely fine grained or a material in which very small crystals are embedded in an amorphous matrix in so produced materials has not been easy on the basis of diffraction basis [10]. Only the supplementary investigations by neutron diffraction can unambiguously confirmed that the phases produced by MA are truly amorphous. The milled powder is finally heat treated to obtain the desired microstructure and properties. Annealing leads to grain growth and release of microstrain [8].

In MA elemental powders are used as the starting materials whilst in high energy ball milling the starting material is an alloy of the desired composition.

3. NANOSINTERING

For certain nanomaterials application, sintering of powders while retaining grain sizes in the nanometer scale range becomes a critical processing step. Fully dense specimens with

nanosize features are most important for magnetic, electrochemical as well as engineering applications. The key of nanopowder consolidation is the retention of initial metastable structures. The metastabilities can be divided into three main categories [11]: compositional (extended solution ranges), structural or topological (alternate crystal structure or amorphous phases) and morphological (finely divided structures). Sintering of nanopowders is significantly enhanced. For example, sintering of nanoparticles indicated depressed sintering onset temperatures (0.2–0.3 Tm) as compared to conventional powders (0.5–0.8 Tm).

4. EXPERIMENTAL DETAILS

4.1. Preparation of the materials

Mechanical alloying was performed under argon atmosphere using a SPEX 8000 Mixer Mill. The starting materials used were high purity powders. The studied mixtures were first mixed by ball milling with hard steel balls for different times (see text for details) and then compacted. Finally, green compacts were heat treated at high temperatures for different times in the mixture of argon – 5% hydrogen gases.

4.2. Characterization

X-ray diffraction (XRD) was employed to study the effect of mechanical alloying and of any subsequent heat treatment on the phases present. XRD were performed using a X-ray powder diffractometer with Co-K_α radiation. The effect of the different processing methods on sinterability was assessed by density (Archimedes method) and Vickers' hardness measurements. Vickers' hardness was tested on polished surfaces under a load of 200g. Scanning electron microscope (SEM) and energy dispersive spectrometry (EDS) techniques were used to study the microstructure and morphology of the samples. An electrochemical corrosion polarization test cell was used for in vitro potentiodynamic corrosion test in 1M H_2SO_4 distilled water solution. Saturate calomel solution was used as the reference electrode and graphite as the counter electrode. Corrosion potentials and corrosion current densities were determined by Tafel extrapolation methods.

5. PROPERTIES OF SELECTED NANOSTRUCTURED MATERIALS

5.1. The manufacturing of titanium-hydroxyapatite nanocomposites

XRD patterns of the Ti-10vol% HA mixture mechanically alloyed for different time and heat treated are shown in Fig. 1.

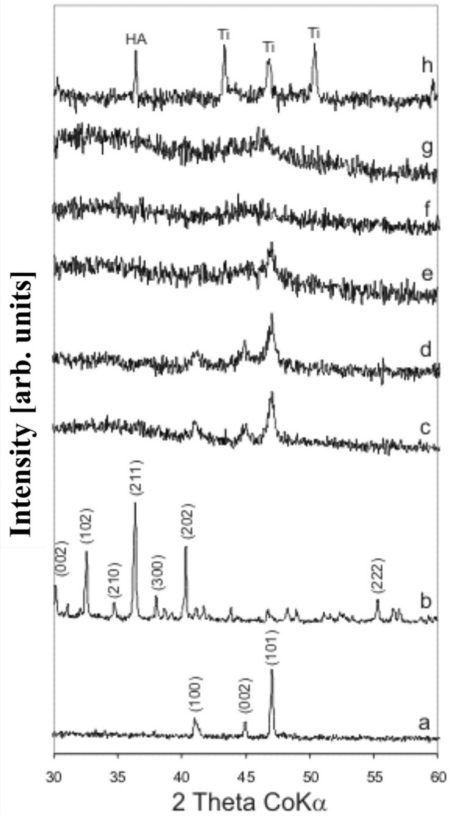

Fig. 1. XDR spectra of Ti and HA powders mechanically alloyed for different times: (a) Ti-0 h, (b) HA-0 h, (c) 1h, (d) 3h, (e) 5h, (f) 10h, (g) 43h, (h) after annealing at 1150°C for 2h

Rys. 1. Dyfraktogramy rentgenowskie mielonych proszków Ti-HA dla różnych czasów trwania procesu MA : (a) Ti-0 h, (b) HA-0 h, (c) 1h, (d) 3h, (e) 5h, (f) 10h, (g) 43h, (h) po obróbce cieplnej 1150^{0}C/2h

Fig. 1a and 1b show XRD patterns of the starting materials. During mechanical alloying the originally sharp diffraction lines of Ti and HA gradually become broader and their intensity decreases with milling time (Fig. 1c, d, e). The peak broadening represents a reduc-

tion in the crystallite size and an increase in the internal strain in the MA materials. The powder mixture milled for more than 43h has transformed completely to an amorphous phase (Fig. 1f). Formation of the nanocrystalline composite material was achieved by annealing of the amorphous material. After thermal treatment the peaks of titanium are shifted in direction of higher 2Θ values. The unit cell volume of started Ti powders was decreased of about 15% for comparison with the Ti-10vol% HA material. The grain size of heat treated Ti-10vol% HA composite determine by Scherer methods is about 30-40 nm.

The influence of the milling time and annealing time on density and hardness of Ti-10vol% HA composite are given in Figs. 2 and 3. Fig. 2 shows that Vickers' hardness of the sintered samples declines for 10-20h of MA due to the lower density. But for 43h of MA, density and hardness are considerably increased. Vickers' hardness of Ti-10vol% HA after 43h of MA and annealing composite is five times higher (~1300 HV) than that of microcrystalline titanium (250 HV). As shown in Fig. 3 the Vickers' hardness of the sintered composite (43h of MA) is changed in function of annealing time at 1150 ºC. Vickers' hardness increase with increase of the annealing time from 1300 HV for 0.25h of heat treated to 1500 HV for 2h of heat treated [12].

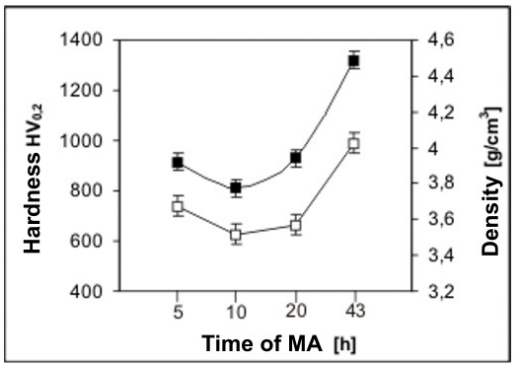

Fig. 2. Vickers' hardness (■) and density (□) in function of milling time (annealing 1150 °C/2h)

Rys. 2. Wpływ czasu mieszania MA na twardość (■) i gęstość (□) próbek (obróbka cieplna 1150 °C/2h)

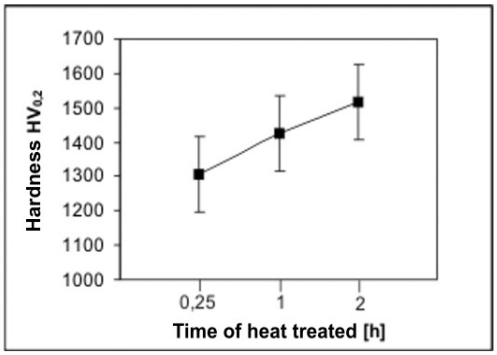

Fig. 3. Vickers' hardness in function of annealing time at 1150° (43h of MA)

Rys. 3. Wpływ czasu obróbki cieplnej (1150°) na twardość próbki po 43h MA

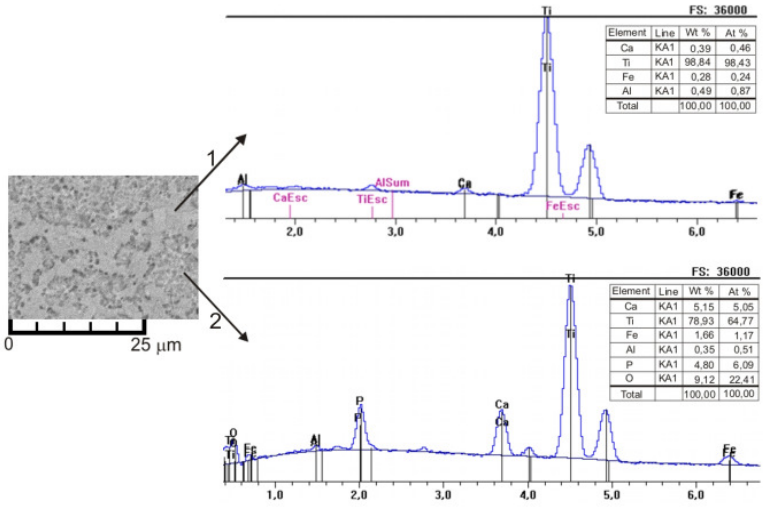

Fig. 4. EDS spectra of surface of the Ti–HA nanocomposite mechanically alloyed for 43h and heat treated at 1150 °C for 2h

Rys. 4. Mikroanaliza rentgenowska powierzchni nanokompozytu Ti-HA otrzymanego metodą MA (4 h) i obrobionego cieplnie w temperaturze 1150 °C w czasie 2h

The SEM morphologies and EDS spectra of the Ti-10vol % HA nanocomposite surfaces are shown in Fig. 4. This composite consist of two matrixes rich in titanium included HA particles (matrix 2) and calcium (matrix 1).

Fig. 5 shows the potentiodynamic polarization curves of the Ti and Ti-10vol% HA composite. The corrosion current densities and corrosion potentials were determined from the potential polarization curves by Tafel extrapolation method. These results are shown in Table 1. According to Table 1, the Ti-10vol% HA composite was more corrosion resistant ($I_C = 1{,}1 \cdot 10^{-6}$) than the microcrystalline Ti ($I_C = 2{,}7 \cdot 10^{-5}$). Besides, the polarization curve (Fig. 5a) of the composites was wider passive range, compared with curve (b), which is the pure titanium.

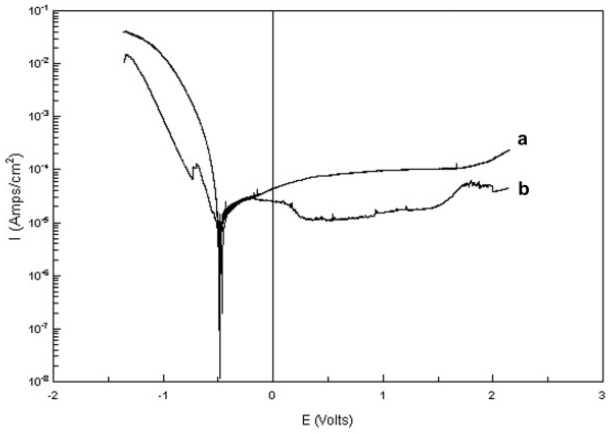

Fig. 5. Potentiodynamic polarization curves of: (a) Ti-10vol% HA and (b) Ti in the 1M H_2SO_4 distilled water solution

Rys. 5. Potenciodynamiczne krzywe polaryzacji otrzymane dla (a) Ti-10vol% HA i (b) Ti w 1M roztworze wodnym H_2SO_4

Table 1. Mean values of corrosion current densities and corrosion potentials of Ti-10vol% HA and Ti

Tablica 1. Średnia wartość gęstości prądów korozyjnych i potencjałów korozyjnych dla Ti-10vol% HA i Ti

	I_C [Amp/cm^2]	E_C [V]
Ti	$2{,}7 \cdot 10^{-5}$	-0.47
Ti-10vol % HA	$1{,}1 \cdot 10^{-6}$	-0,48

5.2. Austenitic nanocrystalline nickel-free stainless steel

The XRD patterns on Fig. 6 are representative of a Fe74Cr24Mo2 alloy after MA, annealing and nitrogenation under different conditions. First diffraction pattern shows a mixture of initial powders (Fig. 6a). After 48h of MA the alloy had decomposed into an amorphous phase, and nanocrystalline α-Fe (Fig. 6b). Heat treatment performed after MA process results in crystallization into ferritic phase (Fig. 6c). Then, compacted material was firstly nitrided at 1050 ^oC (Fig. 6d) which was not sufficient temperature to achieve austenitic phase. Nitrogen absorption carried out at 1200^oC results in phase transformation from ferritic to fully austenitic (Fig. 6e) [13]. Crystallite size of so produced material, 27 nm, was estimated by Scherrer's method.

Changes of size and shape of the mechanically alloyed powder mixtures as a function of milling time was done by the SEM technique (Fig. 7). Starting materials that forms the microstructure during MA (Fig. 7a, 7b, 7c) were mixed together (Fig. 7d). The lamellar structure is increasingly refining during further mechanical alloying (Fig. 7e) which leads to true alloy formation (Fig. 7f). After alloying samples shows cleavage fracture morphology and inhomogenous size distribution (Fig. 7g). Many small powders tends to agglomerate. Bulk FeCrMo material with 98% theoretical density was prepared by sintering (750 ^oC/0.5 h) and then nitrided at 1200 ^oC for 24 hours (Fig. 7h).

EDX analysis (Fig. 8) for Fe74Cr24Mo2 alloy confirms that in the material's matrix there is 74% of iron, 20% of chromium and 3% of molybdenium. Content of nitrogen in this case is 0.56%, there is also 2.47% content of oxygen. Oxygen content in syntesized materials was carried out using XPS method. At the grain boundaries one can observe small content of manganese and increase of oxygen content to 7% at. Dependent on region, nitrogen content is changing from 0 to 2.16% due to diffusion effects.

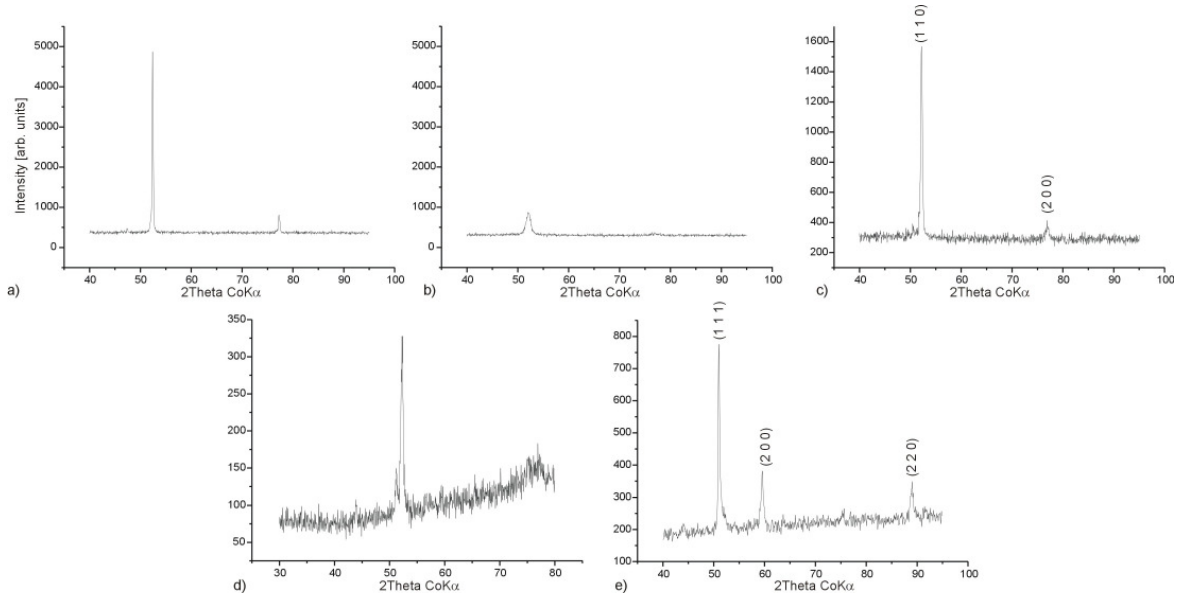

Fig. 6. X-ray diffraction spectra of produced material: a) mixture of initial powders, b) after 48h of MA, c) after heat treatment, d) after nitrogen absorption at 1070 ^{o}C, e) after nitrogen absorption at 1200 ^{o}C

Rys. 6. Dyfraktogramy rentgenowskie otrzymanego materiały: a) mieszanina proszków wyjściowych b) po 48h trwania mechanicznej syntezy, c) po obróbce cieplnej, d) po azotowaniu w temp. 1070 ^{o}C, e) po azotowaniu w temperaturze 1200 ^{o}C

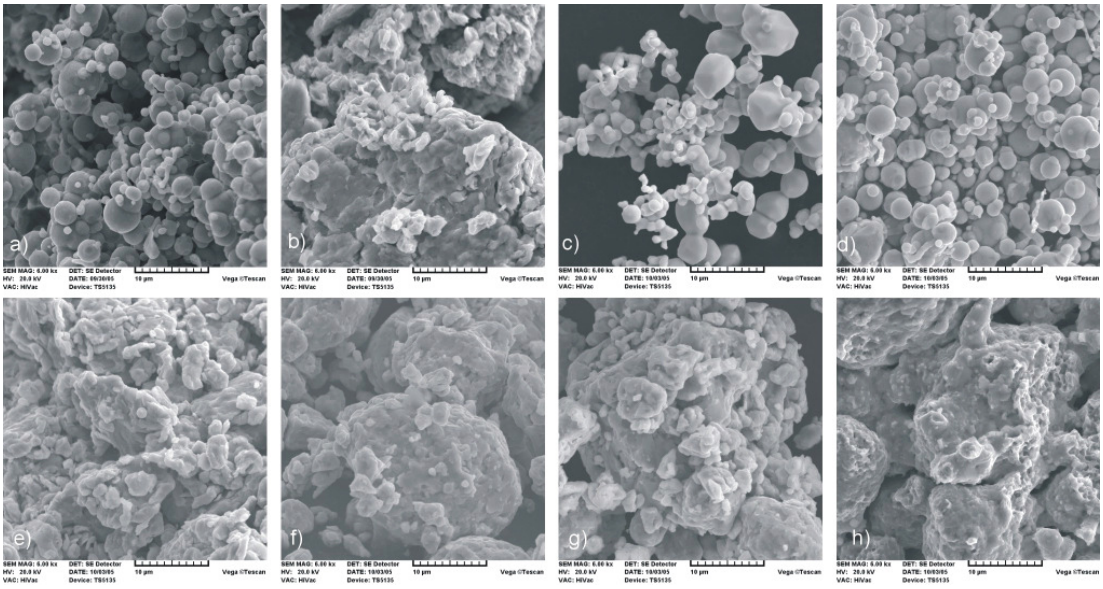

Fig. 7. SEM microstructures: a) Fe powder, b) Cr powder, c) Mo powder, d) mixture of initial powders, e) material after 1h of MA, f) material after 48h of MA, g) material after heat treatment, h) final bulk material after nitrogen absorption

Rys. 7. Zdjęcia SEM a) Fe, b) Cr, c) Mo, d) mieszanina proszków wyjściowych, e) po 1h trwania procesu MA, f) po 48h trwania procesu MA, g) po obróbce cieplnej, h) finalny materiał po azotowaniu

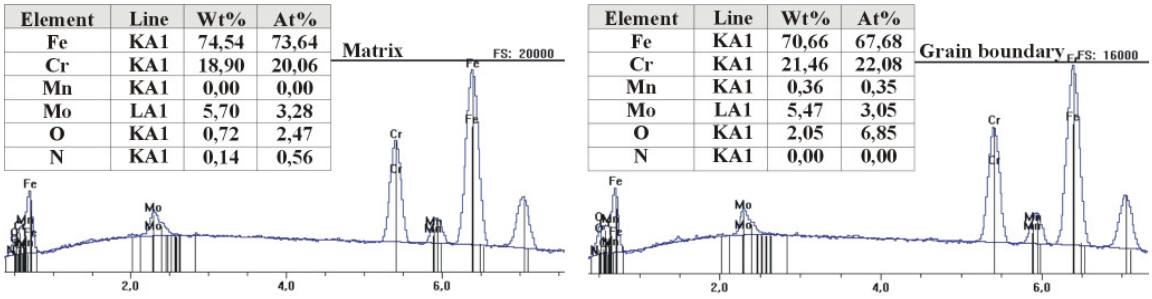

Fig. 8. EDX analysis in matrix and at the grain boundary

Rys. 8. Analiza EDS osnowy oraz granicy międzyziarnowej

The microhardness of the final bulk material was studied using Vickers method and the results are presented on Fig. 9. Compared with A240 commercial austenitic stainless steel (195 $HV_{0.2}$), pure titanium (266 $HV_{0.2}$) and TiNi alloy (279 $HV_{0.2}$) microhardness of sintered nanocrystalline austenitic nickel-free nitrogen containing stainless steel obtained by mechanical alloying is significantly higher (378 $HV_{0.2}$). The result is almost two times greater than in austenitic steel obtained by conventional methods. This effect is directly connected with structure refinement and obtaining of nanostructure.

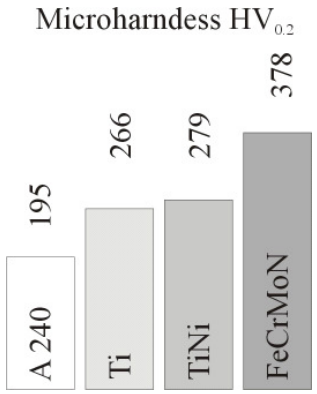

Fig. 9. Microhardness of produced FeCrMoN material compared to A240 stainless steel, pure titanium and TiNi alloy

Rys. 9. Mikrotwardość otrzymanego materiału FeCrMoN w porównaniu do mikrotwardości stali nierdzewnej A240, czystego tytanu oraz stopu TiNi

5.3. MoS_2 nanoparticles

XRD spectra of studied Mo-S mixture (60 wt % of Mo, 40 wt % of S, before and after MA) are presented in Fig. 10. XRD spectra show that the originally sharp diffraction lines of S become broader and their intensity decreases. Simultaneously, insignificant broadening of Mo diffraction lines is observed. Vanishing of diffraction lines of S could result from amorphization of S or forming of solid solution of S in Mo. After 75h duration of MA process, the diffraction lines of S disappeared (Fig. 10d).

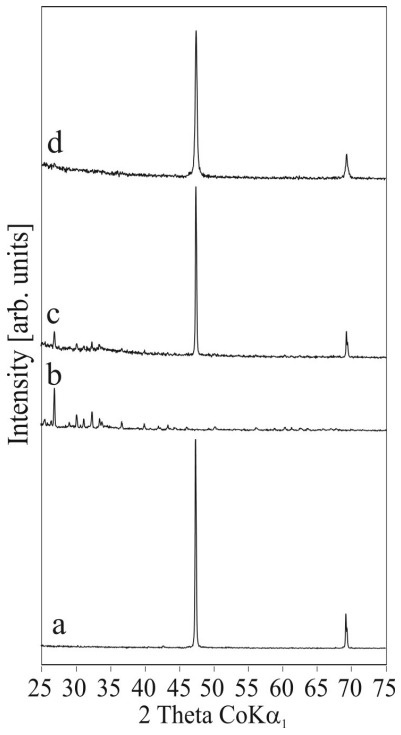

Fig. 10. XRD spectra of a mixture Mo and S powders mechanically alloyed for different time: (a) pure Mo, (b) pure S, (c) after MA 0 h (elemental powder mixture), (d) after MA 75h

Rys. 10. Dyfraktogramy rentgenowskie mieszaniny Mo i S dla różnych czasów trwania Procesu MA : (a) Mo, (b) S, (c) 0 h (mieszanina proszków wyjściowych), (d) po 75h MA

Lengthening of the milling time up to 150h did not cause any significant changes in the structure of milling powders. As-obtained powders were consequently heat treated at 900 °C for 5, 10, 25 and 60 minutes. The mixture of Mo and S (milling time of 15 minutes) were submitted to similar heat treatment. Annealing changes the structure of studied powders. As a result hexagonal structure of MoS_2 was obtained [14]. Influence of heat treatment on the structure of powders is shown in Fig. 11.

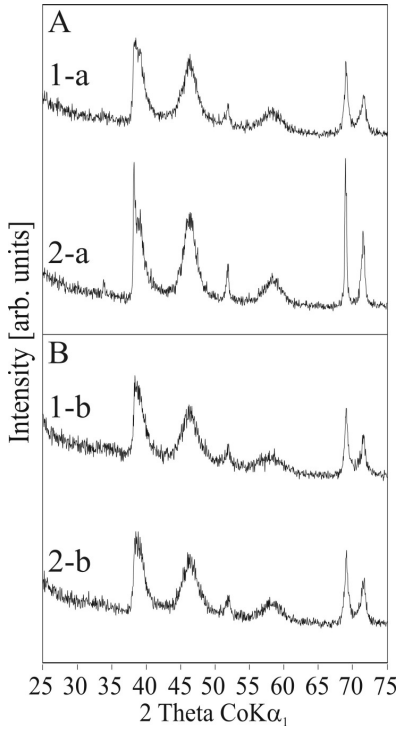

Fig. 11. XRD spectra of a mixture Mo and S
A – produced by mechanical alloying followed by annealing: (1-a) 900 °C/5 minutes (2-a) 900 °C/25 minutes
B – only annealing: (1-b) 900°C/5 minutes
(2-b) 900 °C/25 minutes
Rys. 11. Dyfraktogramy rentgenowskie mieszaniny M i S
A – poddanych MA i obróbce cieplnej: (1-a) 900 °C/5 min., (2-a) 900 °C/25 min.
B – poddanych wyłącznie obróbce cieplnej: (1-b) 900 °C/5 min., (2-b) 900 °C/25 min

The XRD patterns show a significant broadening of diffraction lines. The time factor did not have any major impact on the final structure of sulphide powders. Only insignificant sharpening of diffraction lines for powders obtained by MA process followed by annealing at 900 °C for 60 minutes was observed. Regardless similar XRD patterns, sulphide MoS_2 displayed different morphology. This is related to the applied method. The SEM technique was used to analyze the changes in the size and shape of particles at different stages of the process.

Fig. 12 shows the morphology of obtained sulphide. Pictures A, B and C present the sulphide generated by 75h MA and followed by annealing at 900 °C for 5, 10, 25 minutes, respectively. Picture D, E and F show the sulphide obtained without applying MA but with the same annealing parameters as above. It has been observed that the sulphide obtained from Mo and S mixture without applying MA consists of agglomerates whose size is a few μm. The annealing time did not change the size of the agglomerates. The morphology of sulphides produced by MA and annealing at 900 °C for 5 minutes is similar to the morphology of sulphides obtained only by annealing at 900 °C for 5 minutes (Fig. 12 A and D). However, in the case of the sulphide obtained by MA, heat treatment affects the morphology of powders.

The extension of annealing time leads to the increase in the number of nanoplate-shaped particles. The sulphide is composed solely nanoplates after 25 minutes of annealing. Their average thickness was about 50 nm. The SEM analysis showed that 60-minute annealing process did not cause any major changes in the morphology of sulphide. It was found that MA process significantly influenced the morphology of sulphide. A detailed explanation of the influence of MA process on the form of sulphide requires further comprehensive research. It appears that factors conducive to the formation of nanoplates are lattice defects caused by MA process, and sulphur solid solution formed in Mo in the duration of the process.

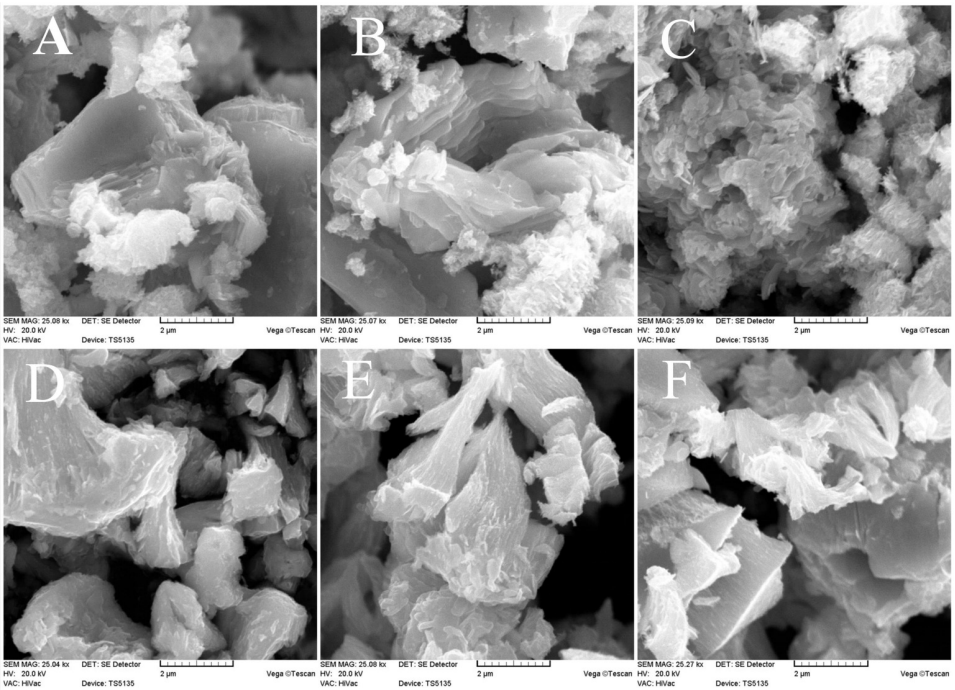

Fig 12. The morphology of studied powders (see text for details)

Rys. 12. Morfologia otrzymanych proszków (opis w tekście)

6. CONCLUSION

It has been shown that mechanical alloying process is a viable processing route for the synthesis of nanoscale metallic engineering materials.

The studies show, that the Ti-HA nanocomposite has been successfully developed by mechanical alloying and powder metallurgical process. Comparing with microcrystalline Ti, Ti-10vol% HA composite has higher Vickers' hardness and corrosion resistance. Ti-HA composite is a promising biomaterial for use as hard tissue replacement implants.

A nanocrystalline austenitic nickel-free nitrogen containing stainless steel samples were produced by means of the MA process and nitrogen absorption. Microhardness test showed that obtained material exhibits Vickers microhardness as high as 378 $HV_{0.2}$, which is about two times higher than that of a conventional austenitic stainless steel. This is due to the structure refinement and the transformation into nanostructured material, achieved by very cheap and successive MA method. According to existing conceptions, decreasing of material's crystallites size to nanometric scale allows to achieve much better mechanical properties (e.g. microhardness) compared to conventional materials. With regard to austenitic stainless steels it could help to obtain better biomedical implants (e.g. stents) with better mechanical properties, corrosion resistance and biocompatibility.

Other mechanical and corrosion properties as well as cytocompatibility of produced material will be a part of the further research. There are many premises that this kind of material has good corrosion resistance and fabrication properties (e.g. weldability and formability) combined with higher cytocompatibility than in 316L stainless steels. It is reported that nitrogen absorption treatment contributes to the higher corrosion resistance in the presence of wear.

The research results show that the MA process enables synthesis of MoS_2 nanopowders. Powders which were subjected to MA process followed by annealing obtain nanoplate shape. It has been proved that the duration of heat treatment of powders generated by MA process is a significant factor affecting the morphology of sulphide. The powder exposed to annealing at 900 ^{o}C for 25 minutes obtained the nanoplate form of an average

thickness of 50 nm. As-generated MoS_2 could find application in the production of nanocomposites which could be employed in the manufacturing of machine parts with enhanced tribological properties.

Generally, the mechanical properties of obtained nanoscale metallic materials show considerable increase in comparison to the values found in conventionally (microcrystalline) materials.

ACKNOWLEDGEMENTS

Support for this work was provided by the Poznan University of Technology, Faculty of Mechanical Engineering and Management

Materiały prezentowane były na Seminarium pt. „New materials for advanced applications", 18-19.09.2006 r. Poznań-Wąsowo.

REFERENCES

[1] M. Jurczyk, The progress of nanocrystalline hydride electrode materials, Bull. Pol. Ac.: Tech. 52(1) (2004) 67-77.

[2] M. Jurczyk, Remanence Enhanced Nd2Fe14B/α-Fe and Nd(Fe,Mo)12Nx/α-Fe type Magnetic Powders Produced by High-Energy Ball-Milling, J. Alloys Comp. 235 (1996)232-236.

[3] M. Jurczyk, L. Smardz, K. Smardz, M. Nowak, E. Jankowska, Nanocrystalline LaNi5-type electrode materials for Ni-MHx batteries – invited, J. Solid State Chem. 171 (2003)30-37.

[4] J. Richert, M. Richert; A new method for unlimited deformation of metals and alloys, Aluminium 62 (1986)604-607.

[5] K.J. Kurzydłowski, M. Richert, J. Richert, J. Zasadziński, Effect oh non-conventional large deformation on microstructure and properties of metals, Int. Workshop on Processing and Characterisation of Nanomaterials, Warsaw, Poland, 2003 – CD-Rom.

[6] A. Dollar, S. Dymek, Microstructure and high temperature mechanical properties of mechanically alloyed Nb3Al-based materials, Intermetallics 11 (2003)341-349.

[7] M. Jurczyk, Nanomateriały, Wydawnictwo Politechniki Poznańskiej, Poznań 2001.

[8] M. Jurczyk, Mechaniczna synteza, Wydawnictwo Politechniki Poznańskiej, Poznań 2003.

[9] J.S. Benjamin, Mechanical alloying, Sc. American 234 (1976) 40-57.

[10] C. Suryanarayna, Mechanical alloying, Progr. Mater. Science 46 (2001) 1-184.

[11] J.R. Groza J.R., Nanosintering, NanoStructured Mater. 12 (1999) 987-992.

[12] K. Niespodziana, K. Jurczyk, M. Jurczyk, Synteza bionanomateriałów kompozytowych typu tytan–hydroksyapatyt, Inż. Materiałowa 3 (2006) 636-639.

[13] M. Tulinski, K. Jurczyk, M. Jurczyk, Przemiana fazowa bezniklowych ferrytycznej w austenityczną w azotowanych bezniklowych stalach nierdzewnych, Inż. Materiałowa 3 (2006) 292-295.

[14] M. Nowak, Nanokrystaliczny MoS_2 otrzymany metodą mechanicznej syntezy, Inż. Materiałowa 3 (2006) 640-642